Journal of Applied Science and Education, 2025,
Vol. 05, Iss. 02, S. No. 111, pp. 1-11
ISSN (Online): 2583-1372

Mathematical Modelling and Theoretical Exploration of Hybrid Blood-Nano-fluid Flow in a Stenosed Artery with Magnetization Effect

Anil Kumar[1], Ram Bharat Singh[2], Jyoti Sinha[3] and Akash[4]

[1]Department of Applied Sciences and Humanities, IMS Engineering College, Ghaziabad- 201009, UP, India
[2]Department of Mathematics, Starex University Gurugram-122413, Haryana, India
dranilkumar73@rediffmail.com, rambharat.maths@gmail.com, romjyoti@yahoo.co.in, singh475@gmail.com

How to cite this paper: A. Kumar, R. B. Singh, J. Sinha and Akash, "Mathematical Modelling and Theoretical Exploration of Hybrid Blood-Nano-fluid Flow in a Stenosed Artery with Magnetization Effect," *Journal of Applied Science and Education (JASE)*, Vol. 05, Iss. 02, S. No. 111, pp 1-11, 2025.

https://doi.org/10.54060/a2zjournals.jase.111

Received: 12/02/2025
Accepted: 15/06/2025
Online First: 14/07/2025
Published: 14/07/2025

Abstract

In this study, we investigate the effects of hybrid blood-nano-fluid flow in stenosis arteries under the influence of magnetization. The governing equations are expressed and solved using the standard finite difference method, and the key parameters, such as the flow parameter, Prandtl's number, blood flow rate, and skin friction, are computed to detect the behavior of blood flow in stenosis arteries. The mathematical model uses blood as a Newtonian fluid and assumes that it is two-dimensional (2D).In order to give a thorough understanding of the physiological dynamics, the differences between these parameters are illustrated graphically. The results demonstrate that while a larger nano-particle volume fraction and Prandtl number result in a decrease in blood temperature, an increase in the flow parameter increases velocity. With the tailored use of nanoparticles, nanotechnology displays great promise from a biomedical perspective, especially in chemotherapy. For a more thorough and correct description of blood rheology, this study emphasizes the necessity for future modifications by adding more factors.

Keywords

Mathematical model, impedance, nano- fluid, hybrid blood, shear stress, stenosis.
AMS Subject Classification No. (2020): 76Z05, 92C35

1. Introduction

The cardiovascular system, a fundamental component of circulation, consists of blood, blood vessels, and the heart. The heart's pumping action ensures the continuous flow of blood throughout the body. Nevertheless, blood vessels may undergo narrowing due to plaque deposition or abnormal arterial growth, a condition known as arterial stenosis. Stenosis arteries can result in severe complications, including thrombus establishment, stroke, heart failure, and arrhythmias, posing substantial risks to cardiovascular health. An accumulation of atheromatous plaque along the wall of the endothelium walls causes arterial stenosis, a pathological disease marked by the progressive narrowing of arterial lumina. It is crucial to the physiology of atherosclerosis, a chronic cardiovascular disease characterized by the buildup of fibrous materials, cholesterol, and lipids. This vascular constriction impairs hemodynamic stability, which raises the risk of myocardial infarction, ischemic stroke, and other cardiovascular morbidities as well as impairs perfusion. A fundamental understanding of fluid mechanics is essential for analyzing blood circulation dynamics. Kumar et al. [1] explored the finite element Galerkin approach for a computational analysis of arterial flow and their applications. Kumar et al. [2] developed a computational technique to analyze blood flow in vessels with porous effects. Ali and Das [3] investigated the electroosmotic impact on fractional Jeffrey blood flow with nanolayer-coated tetra-hybrid nanoparticles in a charged stenotic-aneurysm artery. Several researchers [4–6] have conducted both experimental and computational studies to further investigate blood flow mechanics in stenotic arteries. Nanofluids, which are engineered suspensions of nanoparticles within base fluids, have garnered significant attention in biomedical applications.

Many studies have investigated the influence of nanoparticles on blood flow dynamics. Gupta [7] explored the finite element Galerkin scheme for blood flow in vessels under magnetic effects. Shah and Kumar [8] conducted computational studies on blood flow through constricted arteries. The effect of chemical processes and an inclined magnetic field on the slip flow of blood in a tri-hybrid Carreau nano-fluid through a porous, inclined stenosed artery with viscous dissipation was examined by Deshwal et al. [9]. The effects of hybrid nanoparticles have been further investigated [10–13, 19]. Ali et al. [14] investigated their behavior under magnetohydrodynamic (MHD) settings, while Ali et al. [15] investigated their thermal characteristics under circumstances of viscous dissipation and heat flux possessions. Numerical solutions for non-Newtonian hybrid fluid flow in a permeable material when magnetic fields are applied were given by Elgazery [16].

Ahmed and Nadeem [17] examined various nanoparticle types under mild stenosis conditions, deriving exact solutions using the Euler-Cauchy method and presenting results both graphically and in tabular form. Mekheimer et al. [18] emphasized the potential of nanoparticles in cancer treatment, emphasizing their high atomic number and heat-generating properties. They applied the long-wavelength assumption to solve governing equations related to nanoparticle-induced thermal energy. By enhancing the absorption of heat radiation, thermal radiation therapy can assist lower blood flow resistance based on by situations like stenosis and magnetic fields, according to [20]. The action of nano-fluids in stenosed arteries is better unstated thanks to this study, which highlights how crucial it is to take into account various effects while modeling. It aspects into how heat transfer, chemical reactions, pressure gradient variation, and magnetic field effects all work together to affect nano-blood flow in stenosed arteries.[21].

This study is driven by the complex interface among blood pour subtleties and stenotic artery conditions. Advanced mathematical modeling plays a crucial role in analyzing the intricate physiological processes involved and evaluating the impact of stenosis on blood flow. Through the application of mathematical equations, this research offers a detailed assessment of stenotic conditions, providing valuable insights for both theoretical developments and medical applications.

2. Flow Geometry

The following assumptions are made for the mathematical modeling of blood flow through a stenotic artery:

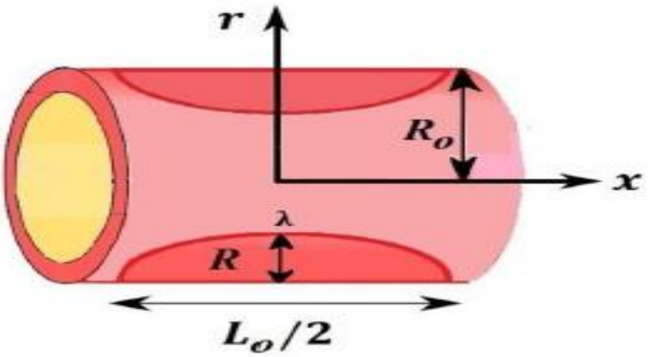

Figure 1. Geometry of Stenosis Artery

i. The study considers blood flow through a stenosis artery featuring a cosine-shaped compression.
ii. Blood is represented as a 2D incompressible Newtonian fluid that is stable.
iii. The stenosis measures $L_0/2$ in length, $2R_0$ in breadth in the unclogged zone, R(x) for the artery radius, and λ for the maximal stenosis altitude.
iv. The r-axis is concerned with vertical flow direction, while the x-axis is concerned with lateral blood flow.
v. The stenosis region is mathematically well-defined as:

$$R[x]=\begin{cases} R_0-\dfrac{\lambda}{2}\left[1+\cos\left(\dfrac{4\pi x}{L_0}\right)\right], & -\dfrac{L_0}{4}<x<\dfrac{L_0}{4} \\ 0, & \text{Otherewise} \end{cases} \tag{1}$$

3. Mathematical Model

A Newtonian hybrid nano-fluid's motion, momentum, and energy limiting reliable margin layer equations are as follows:

$$\frac{\partial(rw)}{\partial x}+\frac{\partial(ru)}{\partial x}=0 \tag{2}$$

$$\left(w\frac{\partial w}{\partial x}+u\frac{\partial w}{\partial r}\right)=\frac{\mu_{hnf}}{\rho_{hnf}}\frac{\partial}{r\partial r}\left(r\frac{\partial w}{\partial r}\right)-Mw, \tag{3}$$

$$\left(w\frac{\partial \mathrm{H}}{\partial x}+u\frac{\partial \mathrm{H}}{\partial r}\right)=\frac{k_{hnf}}{\left(\rho C_p\right)_{hnf}}\frac{\partial}{r\partial r}\left(r\frac{\partial \mathrm{H}}{\partial r}\right) \tag{4}$$

The corresponding boundary conditions are

$$\left.\begin{aligned} &w=0,\ u=0 \text{ and } \mathrm{H}=\mathrm{H}_1 \text{ at } r=R[x] \\ &w'=0,\ H'=0 \qquad \text{at} \qquad r=0. \end{aligned}\right\} \tag{5}$$

where w ' and H' are the partial derivative with respect to r.

Ardahaie et al. [13] determined the somatic characteristics of the nano-fluid.

$$\left.\begin{aligned}
&\rho_{nf}=\rho_f\left\{(1-\phi)+\phi\frac{\rho_s}{\rho_f}\right\},\quad \mu_{nf}=\frac{\mu_f}{(1-\phi)^{5/2}}\\
&\left(\rho C_p\right)_{nf}=\left(\rho C_p\right)_f\left\{(1-\phi)+\phi\frac{\left(\rho C_p\right)_s}{\left(\rho C_p\right)_f}\right\}\\
&\frac{k_{nf}}{k_f}=\frac{k_s+2k_{bf}-2\phi\left(k_{bf}-k_s\right)}{k_s+2k_{bf}+\phi\left(k_{bf}-k_s\right)}
\end{aligned}\right\} \tag{6}$$

and

$$\left.\begin{aligned}
&\rho_{hnf}=(1-\phi_2)\left\{(1-\phi_1)\rho_f+\phi_1\rho_{s_1}\right\}+\phi_2\rho_{s_2},\mu_{hnf}=\frac{\mu_f}{(1-\phi_1)^{5/2}(1-\phi_2)^{5/2}}\\
&\left[\rho C_p\right]_{hnf}=(1-\phi_2)\left\{(1-\phi_1)\left(\rho C_p\right)_f+\phi_1\left(\rho C_p\right)_{s_1}\right\}+\phi_2\left(\rho C_p\right)_{s_2}\\
&\frac{K_{hnf}}{K_f}=\frac{K_{s_1}+2K_f-2\phi_1\left(K_f-K_{s_1}\right)}{K_{s_1}+2K_f+\phi_1\left(K_f-K_{s_1}\right)}\times\frac{K_{s_2}+2K_{nf}-2\phi_2\left(K_{nf}-K_{s_2}\right)}{K_{s_2}+2K_{nf}+\phi_2\left(K_{nf}-K_{s_2}\right)}
\end{aligned}\right\} \tag{7}$$

Table 1. Equation (8) provides the expression ζ that corresponds to w and u, promising that equation (2) of continuity is satisfied [12].

Material	Chemical symbol	Density	Heat capacity of the fluid	Thermal conductivity
Blood	-	1054	3518	1.53
Aluminum Oxide	Al_2O_3	3975	767	40.4
Copper	C_u	8940	389	400

Table 1. Composition of Blood Fluid and Hybrid Nanoparticles with Experimental Properties.

$$w=r^{-2}\frac{\partial\zeta}{\partial r}, \tag{8}$$

Then, transforming to equations (3) and (4), we obtain

$$\frac{1}{r}\frac{\partial\zeta}{\partial r}\frac{\partial}{\partial x}\left(\frac{1}{r}\frac{\partial\zeta}{\partial r}\right)-\frac{1}{r}\frac{\partial\zeta}{\partial x}\frac{\partial}{\partial r}\left(\frac{1}{r}\frac{\partial\zeta}{\partial x}\right)=\frac{\mu_{hnf}}{\rho_{hnf}}\frac{\partial}{r\partial r}\left(\frac{\partial^2\zeta}{\partial r^2}-\frac{1}{r}\frac{\partial\zeta}{\partial r}\right)-M, \tag{9}$$

$$\left(\frac{1}{r}\frac{\partial\zeta}{\partial r}\right)\frac{\partial \mathrm{H}}{\partial x}-\left(\frac{1}{r}\frac{\partial\zeta}{\partial x}\right)\frac{\partial \mathrm{H}}{\partial r}=\frac{k_{hnf}}{\left(\rho C_p\right)_{hnf}}\frac{\partial}{r\partial r}\left(r\frac{\partial \mathrm{H}}{\partial r}\right), \tag{10}$$

where M is Hartmann number.

4. Numerical Analysis

The spatial discrete form of the governing equation may still be obtained using the finite difference scheme.
Using (7) and (8), we obtain

$$w=\frac{w_0 x}{L_0}G'(\eta),\ \ u=-\frac{R}{r}\sqrt{\frac{w_0 u_f}{L_0}}F(\eta),\eta=\frac{r^2-R^2}{2R}\sqrt{\frac{w_0}{u_f L_0}},\theta(\eta)=\frac{\mathrm{H}-\mathrm{H}_0}{\mathrm{H}_1-\mathrm{H}_0},$$

$$\zeta=\sqrt{\frac{u_0 x^2 v_f}{L_0}}RF(\eta) \tag{11}$$

where $X=\frac{\tilde{x}}{L_0}$ and the equation.

The spatially discrete form of the governing equations is obtained using a finite difference technique. The semi-discretized governing equations are given by.

$$\frac{1}{B_1 B_2}\left\{(1+2\gamma\eta)\left(\frac{G_{i+3}-2G_{i+2}+3G_{i+1}-G_i}{h^3}\right)+2\gamma\left(\frac{G_{i+2}-2G_{i+1}+G_i}{h^2}\right)\right\}$$
$$+G\left(\frac{G_{i+2}-2G_{i+1}+G_i}{h^2}\right)-Gr^2-M=0 \tag{12}$$

where $B_1=(1-\phi_1)^{5/2}(1-\phi_2)^{5/2}, B_2=\left[(1-\phi_2)\left\{(1-\phi_1)+\phi_1\frac{\rho_{s_1}}{\rho_f}\right\}+\phi_2\frac{\rho_{s_2}}{\rho_f}\right].$

$$\frac{1}{\Pr B_3}\left\{(1+2\gamma\eta)\left(\frac{\theta_{i+2}-2\theta_{i+1}+\theta_i}{h^2}\right)+2\gamma\left(\frac{\theta_{i+1}-\theta_i}{h}\right)\right\} \tag{13}$$
$$+G\left(\frac{\theta_{i+1}-\theta_i}{h}\right)-\left(\frac{G_{i+1}-G_i}{h}\right)\theta=0$$

Where $B_3=\frac{k_{hnf}}{k_f}\left[\left\{(1-\phi_2)\left\{(1-\phi_1)+\phi_1\frac{(\rho C_p)_{s_1}}{(\rho C_p)_f}\right\}+\phi_2\frac{\rho_{s_2}}{\rho_f}\right\}+\phi_2\frac{(\rho C_p)_{s_2}}{(\rho C_p)_f}\right].$

and $\frac{\partial v}{\partial t}=\frac{{v_i}^{n+1}-{v_i}^n}{\Delta t},\quad \frac{\partial v}{\partial x}=\frac{{v_i}^{n+1}-{v_i}^n}{\Delta x}+O(\Delta x)^2.$

The non-dimensional form of equation (1) is

$$f=\begin{cases}1-\dfrac{\in}{2}\{1+\cos(4\pi\tilde{x})\}, & -\dfrac{1}{4}<\tilde{x}<\dfrac{1}{4}\\ 1, & \text{Otherwise}\end{cases} \tag{14}$$

Where $f=\dfrac{R(x)}{R_0}$ and $\in=\dfrac{\lambda}{R_0}$ is the dimensionless measure of stenosis in reference artery.

The discretized boundary conditions are

$$G(0)=0,\left(\frac{G_{i+1}-G_i}{h}\right)(0)=0,\theta(0)=1 \quad \text{at} \quad \eta=0 \quad , \tag{15}$$

$$\left(\frac{G_{i+2}-2G_{i+1}+G_i}{h^2}\right)(\eta)=0,\ \left(\frac{\theta_{i+1}-\theta_i}{h}\right)(\eta)=0 \quad \text{at} \quad \eta=f. \tag{16}$$

The non-dimensional quantities are given by

$\gamma=\sqrt{\dfrac{\nu_f L_0}{u_0 R^2}}$, $\Pr=\dfrac{k_f}{(\mu C_p)_f}$, ϕ_1 and ϕ_2 nanoparticles concentration of copper aluminum oxide.

The coefficients of skin friction and heat transfer are computed using the following mathematical expressions:

$$C_f=\frac{\tau_u}{\frac{1}{2}\rho_f U_u^2} \tag{17}$$

$$Nu_x=\frac{xq_w}{k_f(T_W-T_\infty)} \tag{18}$$

The shear stress and heat flux are evaluated using the following mathematical expressions:

$$\tau_u=\left\{\mu_{hnf}\left(\frac{\partial w}{\partial r}\right)\right\}_{r=R} \tag{19}$$

$$\tau_W=\left\{-k_{hnf}\left(\frac{\partial T}{\partial r}\right)\right\}_{r=R} \tag{20}$$

The corresponding dimensionless quantities are

$$\mathrm{Re}_x^{1/2} C_f=\frac{1}{(1-\phi_1)^{5/2}(1-\phi_2)^{5/2}}G''(0) \tag{21}$$

$$\mathrm{Re}_x^{-1/2} Nu_x=-\frac{k_{hnf}}{k_f}\theta'(0) \tag{22}$$

where $\mathrm{Re}_x^{-1/2}$ is the Reynolds number.

5. Computational solution

Utilizing the MATLAB bvp4c approach, the numerical solution of equations (12) and (13) is found. Boundary values issues for ordinary differential equations are resolved by MATLAB bcp4c. A graphic representation of the temperature and velocity profile values is produced.

6. Results and Discussion

Although our primary goal has been to investigate stenosis artery with magnetization effect, the stable cases are also of interest. The results have been numerically evaluated for various parameter combinations considered in the solution. This study investigates blood flow through a stenosis artery incorporating hybrid nanoparticles. The influence of different parameters on the stenosis artery is examined comprehensively.

The relationship between temperature and Prandtl number (Pr) is depicted in Figure 2. According to the graphical results, temperature decreases as Pr rises. A diminishing trend as the concentration of nanoparticles increases is depicted in Figure 3, which shows the effect of nanoparticles on the temperature field. The effect of y on blood temperature is shown in Figure 4, where larger values of y result in higher blood temperatures.

Figure 5 illustrates how nanoparticles affect the velocity profile.The effects of y on the velocity distribution are seen in Figure 6. Blood velocity rises as y values increase. The effects $F(\eta)$ on velocity distribution $F'(\eta)$ are depicted in figure 7. The variations in skin friction caused by variations in the flow parameter and nano-particle volume percentage are depicted in figure 8. The effect of the heat transfer coefficient is shown in figure 9, where the curve shows a declining trend.

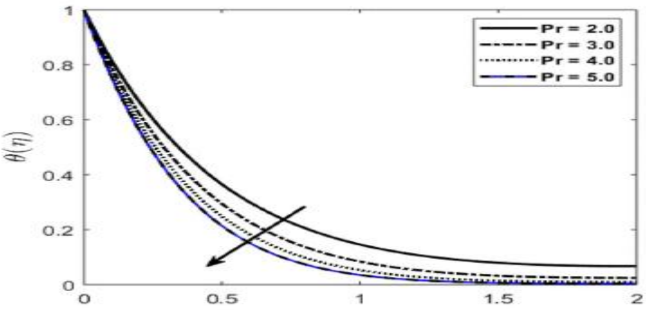

Figure 2. Plot diagram of consequences of $\theta(\eta)$.

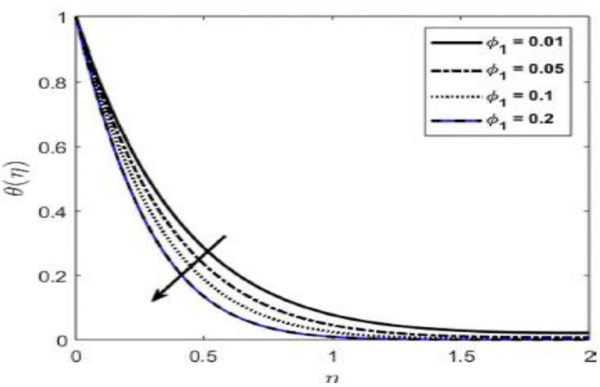

Figure 3. Diagrams depict the volume proportion of nanoparticles on $\eta\theta(\eta)$.

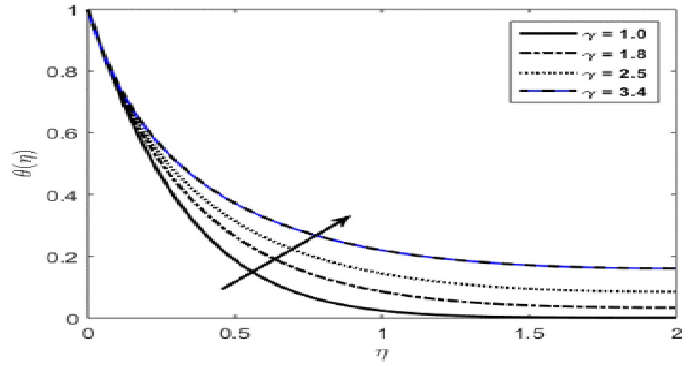

Figure 4. Plot diagram of velocity profile against γ on η θ(η).

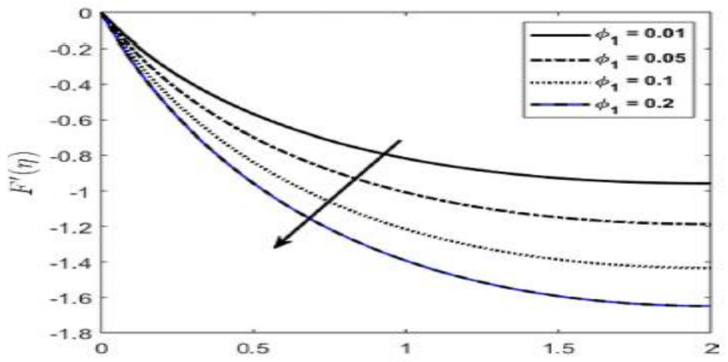

Figure 5. Plot diagram of velocity profile against volume fraction on η ϑ'(η).

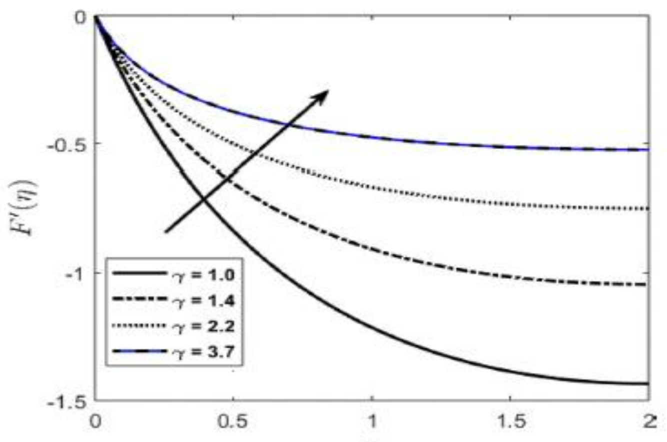

Figure 6. Plot diagram of velocity profile against γ on ηf'(η).

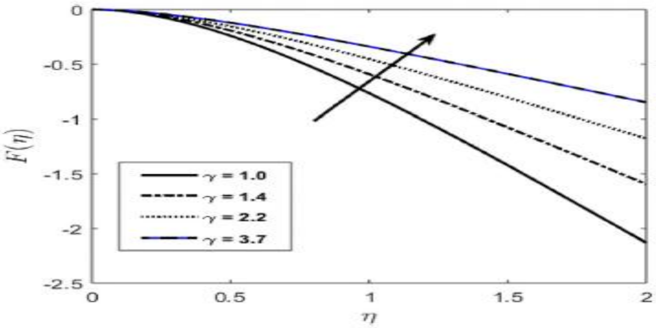

Figure 7. Plot diagram of velocity profile against γ on η f(η).

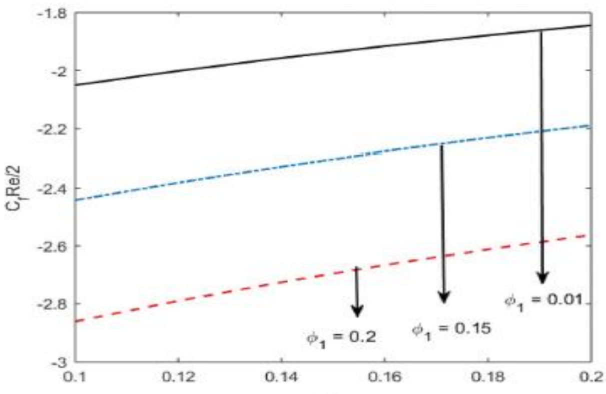

Figure 8. Plot diagram of variation of nanoparticle volume fraction and γ on C_f .

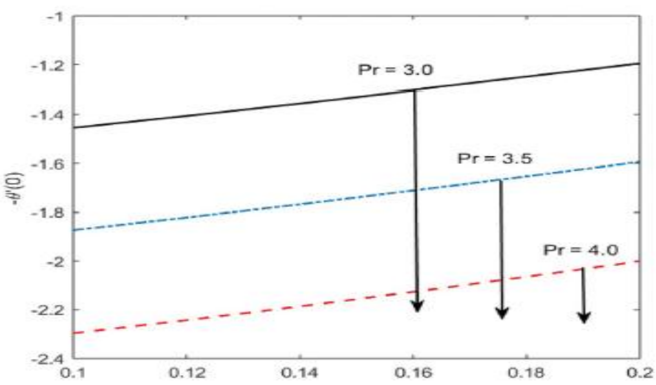

Figure 9. Plot diagram of consequences of Pr and γ on Nu_x .

Table 2. Representation of Numerical Values for Nu with γ and Ø

γ	Temperature field	Dimensionless parameter = 1/2(skin friction coefficient x Reynolds number
0.11	0.012	-2.1505
0.13	0.00	-2.1022
0.15	0.00	-1.9011
1.00	0.00	-2.1509
0.00	0.17	-2.5321
0.00	0.21	-2.2568

7. Conclusion

The current of work, we reproduced the magnetization flow of a blood-based hybrid nano fluid which contained copper and gold hybrid nanoparticles. The impacts of stenosis, chemical responses, heat radiation, and viscous dissipation were all included. In this study, hybrid nanoparticles are used to investigate blood flow through a stenosis artery. Modeling intricate fluid dynamics, vessel geometry, and rheological characteristics is essential for the mathematical study of blood flow in stenotic arteries in order to evaluate how flow behavior is affected by constricted passages. In order to obtain computational solutions, a numerical approach has been utilized. The current study's main conclusions are as follows:

i. A higher temperature curve is the result of increasing the flow parameter.
ii. When nanoparticle size and Prandtl number rise, it is feasible to lower fluid temperature. Blood velocity increases with increasing flow parameter values and decreases with changing nanoparticle concentration.
iii. With an increase in the volume proportion of nanoparticles, the skin friction curve falls.
iv. Nusselt number values change with γ and Pr, which impacts the system's heat transmission properties.

References

[1]. Kumar and M. Jain, "Finite element Galerkin's approach for a computational study of arterial flow," *Applied Mathematics and Mechanics*, vol. 22, pp. 1012–1018, 2001.

[2]. A. Kumar, C. L. Varshney, and G. C. Sharma, "Computational technique for flow in blood vessels with porous effects," *Appl. Math. Mech.*, vol. 26, no. 1, pp. 63–72, 2005.

[3]. A. Ali and S. Das, "Electroosmotic influence on fractional Jeffrey blood flow with nanolay-er-coated tetra-hybrid nanoparticles in an electrified stenotic-aneurysm artery," *Computers in Biology and Medicine*, vol. 88, no. 2025.

[4]. A. Ahmed and S. Nadeem, "Biomathematical study of time-dependent flow of a Carreaunanofluid through inclined catheterized arteries with overlapping stenosis," *J. Cent. South Univ*, vol. 24, pp. 2725–2744, 2017.

[5]. A. Hussain, M. N. Riaz Dar, A. Rehman, F. Hussain, and N. Farooq, "Unconventional wall implications of intertwined stenosis in constrict artery," *Advances in Mechanical Engineering*, vol. 15, no. 3, pp. 1–11, 2023.

[6]. A. Hussain, L. Sarwar, S. Akbar, and S. Nadeem, "Mathematical model for blood flow through the stenosed channel," *Phys. Scr.*, vol. 95, no. 2, p. 025206, 2020.

[7]. A. K. Gupta, "Finite element Galerkin's scheme for flow in blood vessels with magnetic effects," *Int. J. Appl. Syst. Stud.*, vol. 2, no. 3, p. 284, 2009.

[8]. S. R. Shah, and R. Kumar, "Mathematical modeling of blood flow with the suspension of nanoparticles through a tapered artery with a blood clot", *Front. Nanotechnol*, 2020.

[9]. J. Deshwal, S. Chaudhary, and R. Kumar, "Chemical reaction and inclined magnetic field effects on tri-hybrid Carreau nanofluid slip flow of blood past a porous inclined stenosed artery with viscous dissipation," *Phys. Scr.*, vol. 100, no. 3, p. 035216, 2025.

[10]. N. Abbas, S. Nadeem, and A. Saleem, "Computational analysis of water based $Cu—Al_2O_3/H_2O$ flow over a vertical wedge," *Adv. Mech. Eng,* vol. 12, no. 11, pp. 1–10, 2020.

[11]. A. Ahmed and S. Nadeem, "Effects of magnetohydrodynamics and hybrid nanoparticles on a micropolar fluid with 6-types of stenosis," *Results Phys.*, vol. 7, pp. 4130–4139, 2017.

[12]. S. Nadeem, and S. Ijaz, "Theoretical analysis of metallic nanoparticles on blood flow through stenosed artery with permeable walls," *Phys. Lett. A*, vol. 379, pp. 542–554, 2015.

[13]. S. S. Ardahaie, A. J. Amiri, A. Amouei, K. Hosseinzadeh, and D. D. Ganji, "Investigating the effect of adding nanoparticles to the blood flow in presence of magnetic field in a porous blood arterial," *Inform. Med. Unlocked*, vol. 10, pp. 71–81, 2018.

[14]. A. Ali, S. Saleem, S. Mumraiz, A. Saleem, M. Awais, and D. N. Khan Marwat, "Investigation on TiO2–Cu/H2O hybrid nanofluid with slip conditions in MHD peristaltic flow of Jeffrey material," *J. Therm. Anal. Calorim.*, vol. 143, no. 3, pp. 1985–1996, 2021.

[15]. A. Ali, A. Noreen, S. Saleem, A. F. Aljohani, and M. Awais, "Heat transfer analysis of Cu–Al2O3 hybrid nanofluid with heat flux and viscous dissipation," *J. Therm. Anal. Calorim.*, vol. 143, no. 3, pp. 2367–2377, 2021.

[16]. N. S. Elgazery, "Flow of non-Newtonian magneto-fluid with gold and alumina nanoparticles through a non-Darcian porous medium," *J. Egyptian Math. Soc.*, vol. 27, no. 1, 2019.

[17]. A. Ahmed and S. Nadeem, "The study of (Cu, TiO2, Al2O3) nanoparticles as antimicrobials of blood flow through diseased arteries," *J. Mol. Liq.*, vol. 216, pp. 615–623, 2016.

[18]. K. S. Mekheimer, W. M. Hasona, R. E. Abo-Elkhair, and A. Z. Zaher, "Peristaltic blood flow with gold na-noparticles as a third grade nanofluid in catheter: Application of cancer therapy," *Phys. Lett. A*, vol. 382, pp. 85–93, 2018.

[19]. D. G. Yakubu, M. Abdulhameed, G. T. Adamu, and A. M. Kwami, "A study of fractional relaxation time derivative on blood flow in arteries with magnetic and thermal radiation effects," *Diffus. Found.*, vol. 26, pp. 126–144, 2020.

[20]. J. Prakash and O. D. Makinde, "Radiative heat transfer to blood flow through a stenotic artery in the presence of magnetic field," *Latin American Applied Research*, vol. 41, pp. 273–277, 2011.

[21]. A. S. Dawood, F. A. Kroush, and R. M. Abumandour, "Multi-effect analysis of nanofluid flow in stenosed arteries with variable pressure gradient: analytical study," *SN Applied Sciences*, vol. 5, p. 382, 2023. https://doi.org/10.1007/s42452-023-05567-6